

RASSF1A promotes radiosensitivity in nasopharyngeal carcinoma by promoting FoxO3a and inhibiting the Nrf2/TXNRD1 signaling pathway

Yishimei SI^{1,*}, Linghan MENG^{2,*}, Bingwen ZHANG^{2,*}, Yuanqing WU², Qianming DU³, Jinjing XU^{2,*}, Jianwei QI^{2,*}

¹Department of Otolaryngology Head and Neck Surgery, Sir Run-Run Shaw Hospital, Zhejiang University, Hangzhou, China; ²Department of Otolaryngology, Nanjing First Hospital, Nanjing Medical University, Nanjing, China; ³General Clinical Research Center, Nanjing First Hospital, Nanjing Medical University, Nanjing, China

*Correspondence: xujinjing0101@126.com; qjianwei0202@163.com

Received November 22, 2022 / Accepted October 18, 2023

Radiotherapy is widely used as the first-line treatment for nasopharyngeal carcinoma (NPC). However, the resistance of some patients to treatment lowers its clinical effectiveness. Compared to typical epithelial cells, NPC markedly lowers the Ras-association domain family 1A (RASSF1A) protein expression. RASSF1A overexpression sensitizes NPC cells to radiotherapy. Mechanistically, RASSF1A promotes the expression of Forkhead box O3a (FoxO3a) in the nucleus and inhibits the Nuclear factor E2-related factor 2 (Nrf2) signaling pathway via binding to the Kelch-like ECH-associated protein 1 (Keap1) promoter. Through elevating intracellular ROS levels, RASSF1A overexpression inhibits the expression of thioredoxin reductase 1 (TXNRD1), a crucial Nrf2 target gene, and increases NPC sensitivity to radiation. Immunohistochemical staining of NPC tissue sections revealed that the expression of RASSF1A is negatively correlated with that of TXNRD1. The traditional Chinese medicine component andrographolide (AGP), which induces RASSF1A expression, increased the sensitivity of NPC cells to radiotherapy *in vitro* and *in vivo*. Our findings implied that RASSF1A increases the sensitivity of NPC to radiation by increasing FoxO3a expression in the nucleus, inhibiting the Nrf2/TXNRD1 signaling pathway, and elevating intracellular ROS levels. AGP targets RASSF1A and may be a promising adjuvant sensitizer for enhancing radiosensitivity in NPC.

Key words: NPC; RASSF1A; radiosensitivity; FoxO3a; Nrf2/TXNRD1 signaling pathway

Nasopharyngeal carcinoma (NPC) is a squamous cell carcinoma of the head and neck (SCCHN), which originates in the nasopharyngeal epithelium. It exhibits a unique geographical distribution, mainly occurring in southern China and Southeast Asia, with a worldwide age-standardized rate of 3.0/100,000 in China [1, 2]. Its etiology is mainly associated with the Epstein-Barr virus (EBV), as well as environmental factors, genetic susceptibility, and other factors [3]. Since NPC is very sensitive to radiotherapy, the NCCN Clinical Practice Guidelines stipulate radiotherapy as the standard therapy for early-stage as well as intermediate- to advanced-stage NPC [4–6]. However, increased tumor size, dysregulation of key genes, and reduced oxygen tension may lead to clonal selection and tolerance of tumor cells to radiotherapy [7, 8]. Approximately 20% of patients experience treatment failure due to tumor radioresistance, which results in reduced sensitivity to radiotherapy, leading to treatment resistance and tumor recurrence. Therefore, understanding the molecular mechanism underlying NPC-related radioresistance and identifying therapeutic

targets are important for enhancing treatment outcomes in patients with NPC.

The Ras-association domain family 1A (*RASSF1A*) gene is increasingly attracting attention as a tumor suppressor. It is a common gene, the expression of which is either decreased or silenced in cancer. *RASSF1A* is usually downregulated via promoter methylation and rarely by mutation or deletion [9–11]. *RASSF1A* serves as a signaling pathway hub and plays a critical role in signaling by mediating ERK, Hippo, NF- κ B, IL-6/STAT3, and other related pathways [12, 13]. The *RASSF1A* signaling network may modulate various biological functions, such as cell cycle arrest, apoptosis, autophagy, migration, and regulate the microtubule network [14]. However, studies that have investigated the effects exerted by *RASSF1A* on sensitivity to radiotherapy and the mechanisms underlying such effects are scant.

Andrographolide (AGP), a diterpene lactone compound extracted from *Andrographis paniculata*, is used as an anti-inflammatory herb in traditional Chinese medicine. AGP exerts anticancer activity by inhibiting tumor angiogen-

esis, inducing tumor cell apoptosis, regulating autoimmune mechanisms, and affecting the tumor cell cycle [15–17]. Interestingly, AGP sensitizes cancer cells, such as human laryngeal cancer cells and human colorectal cancer cells, to the therapeutic effects of anticancer drugs, including carboplatin and cisplatin [18–19]. In addition, AGP is correlated with sensitivity to radiotherapy. Research has demonstrated that AGP may increase *RASSF1A* expression [17]. However, studies investigating the association between AGP and cell proliferation, sensitivity to radiotherapy, and mechanisms underlying NPC are unavailable.

Nuclear factor erythroid 2-related factor 2 (Nrf2) is a crucial transcription factor, the ubiquitination and rapid degradation of which is promoted by the Kelch-like ECH-associated protein 1 (Keap1). Normally, in the cytoplasm, Nrf2 is anchored to Keap1. In the presence of ROS, Nrf2 detaches from Keap1, enters the nucleus and binds to antioxidant response element (ARE) sequences, thereby activating downstream gene targets, including thioredoxin reductase 1 (*TXNRD1*), NAD(P)H: quinone oxidoreductase 1 (*NQO1*), and heme oxygenase 1 (*HO-1*) [20]. Recent studies have reported that such activation of Nrf2 is closely linked with the mechanism underlying cancer resistance to chemotherapy. For example, Forkhead box O3a (FoxO3a) reverses the resistance of colorectal cancer cells to 5-fluorouracil (5-FU) by blocking the Nrf2/*TXNRD1* signaling pathway. The Nrf2/Keap1 pathway modulates the radiosensitivity of NPC cells by eliminating ROS [21]. Thus, *RASSF1A* may affect the sensitivity of NPC to radiotherapy by modulating FoxO3a and the Nrf2/*TXNRD1* axis against ROS.

In this study, we investigated the mechanism underlying radiosensitivity in NPC, identified the biological functions of *RASSF1A*, and revealed promising pathways that sensitize NPC to radiation.

Materials and methods

Reagents. Antibodies, including anti-GAPDH (1:10000, ab8245), anti-Lamin A/C (1:20000, ab108595), anti-*RASSF1A* (1:1000, ab23950), and anti- β -tubulin (1:1000, ab78078), were purchased from Abcam (Cambridge, MA, USA). Anti-*TXNRD1* (1:5000, 11117-1-AP) were purchased from Proteintech Group (Wuhan, China); RPMI1640, DMEM, and PBS were obtained from KeyGen Biotechnology (Nanjing, China). Matrigel was purchased from Corning (New York, NY, USA). SYBR Green Master Mix was purchased from Takara Biomedical Technology (Dalian, China). The diaminobenzidine (DAB) and UltraSensitive™ SP IHC Kit were purchased from Maxin Biotechnology (Fuzhou, China).

Cell culture. Human NPC CNE1, HONE1, and C666-1 cells were obtained from the Cell Bank of the Chinese Academy of Sciences (Shanghai, China). The cells were cultured in DMEM (C666-1) and RPMI-1640 (CNE1, HONE1), supplemented with 10% fetal bovine serum

(Procell Life Science&Technology Co., Ltd., Wuhan, China), 100 μ g/ml streptomycin, and 100 U/ml penicillin, and incubated in a 37 °C humidified incubator with 5% CO₂. We added AGP (APEX BIO, Houston, TX, USA) to the culture medium to obtain a concentration of 5 μ M (Supplementary Figure S1). After using this medium to culture cells (HONE1) for two days, we obtained HONE1+AGP. Meanwhile, we used the same dose of dimethyl sulfoxide (DMSO) cultured cells as a control group (HONE1+DMSO).

Cell viability assay. Cell viability was detected via a CCK-8 assay (APEX BIO, Houston, TX, USA). Following radiotherapy using diverse doses (2, 4, 6, and 8 Gy), the cells were seeded in 96-well microplates at a density of 3,000 cells/well. After 48 h, cells were cultured with WST-8 (100 μ l/well) for a further 1.5 h. Cellular dehydrogenase reduces WST-8 tetrazolium salt to an orange formazan product that dissolves in a tissue culture medium. The number of viable cells was estimated using formazan-based absorbance at 460 nm. Here, cell viability = $((A_{\text{treated}} - A_{\text{blank}}) / (A_{\text{control}} - A_{\text{blank}})) \times 100\%$. All experiments were performed thrice.

Western blot analysis. Protein samples were collected and placed in a lysis buffer. The samples were then separated via sodium dodecyl sulfate-polyacrylamide gel electrophoresis (SDS-PAGE). Next, they were transferred to polyvinylidene fluoride (PVDF) membranes (Bio-Rad Laboratories, California, USA). The membranes were blocked with skimmed milk for 1 h to prevent non-specific binding. Subsequently, membranes were incubated overnight with primary antibodies at 4 °C. The membranes were then incubated with HRP-binding secondary antibody for 2 h. A GE ImageQuant LAS 500 system (GE Healthcare, Little Chalfont, Buckinghamshire, UK) with ECL luminescent liquid was used to detect proteins. The relative expression levels of each protein were evaluated via ImageJ software.

Plasmid construction and transfection. *RASSF1A* shRNA and scramble shRNA were synthesized and cloned into an LV3 vector (Hanbio, Shanghai, China). *RASSF1A* was amplified and subcloned into an MSCV-PIG vector to construct an overexpression plasmid. Lipofiter (Hanbio, Shanghai, China) was used to transfect the shRNA and plasmids into cells according to the manufacturer's instructions. The cells were cultured in six-well plates until the achievement of 50–70% confluence; subsequently, 4.0 μ g of plasmid and 4.0 μ l Lipofiter (Hanbio, Shanghai, China) were mixed and added to each well. An empty vector was used as negative control (NC). After 48 h, the mRNA and protein expressions of *RASSF1A* were assessed and the cells were subjected to the following experiments. Following transfection, cells were collected for subsequent experiments. The targeting sequence of shRNA is listed (Supplementary Table S1).

Colony formation assay. A colony formation assay was used to evaluate cell proliferation capacity. The cells were treated with or without AGP (5 μ M) for two days. Cells that stably overexpressed *RASSF1A* or downregulated *RASSF1A*

or the vector were exposed to 0, 2, 4, 6, 8, or 10 Gy (2 Gy/fraction), respectively, using a 6-MV X-ray beam from an Elekta linear accelerator (VARIAN CLINAC IX, CA, USA) at a dose rate of 600 cGy/min. Next, the cells were plated in 6-well microplates at approximately 1,500 cells/well, and cultured for 14 days. The resulting clones were fixed with methanol, stained with crystal violet solution, and automatically counted under a microscope. All experiments were performed in triplicate.

In vivo study. Four-week-old male BALB/c nude mice weighing 18 ± 2 g were purchased from GemPharmatech (Nanjing, China). All mice were fed water and diet *ad libitum* under conditions involving a standard environment and a 12 h light/dark cycle. The Nanjing Medical University's Animal Care and Use Committee approved all mouse-related protocols. HONE1/HONE1-AGP cells (1×10^7) were injected into the subdermal space of mice. When the tumor volume reached approximately 200 mm³, tumors were treated with radiotherapy (4 Gy) thrice a week for two weeks. Tumor volumes were measured daily after the first radiotherapy; Tumor volume = $(L \times W^2)/2$ (L, largest diameter; W, smallest diameter). Mice were treated with an Elekta 6-MV photon linear accelerator. Prior to radiation therapy, each mouse was anesthetized with pentobarbital (40 mg/kg), and a lead shield was used to ensure that only the xenograft tumor was exposed. Radiotherapy was administered on days 1, 3, 5, 8, 10, 12, and 14 at a dose of 4 Gy, which corresponds to a dose rate of 600 cGy/min. Tumor size was measured every 2 days for approximately 2 weeks. Subsequently, the mice were sacrificed, and the tumors were collected for immunostaining analyses.

Flow cytometry. Following radiotherapy, cells were collected for flow cytometry. A ROS assay kit (KeyGen Biotechnology, Nanjing, China) was used to test intracellular ROS levels on the basis of the manufacturer's instructions. Properly diluted DCFHDA (10 μ mol/l) was added to adherent cells that had been incubated for 20 min at 37°C without culture solution. The cells were collected in PBS for flow cytometry analysis aimed at estimating ROS levels. The mean fluorescence intensity was calculated after correcting for autofluorescence, and the fold change was calculated. FACS Calibur flow cytometry (BD Biosciences, Franklin Lakes, NJ, USA) was performed and the data were analyzed via FlowJo software (Version X; TreeStar, Ashland, OR, USA).

Tissue immunohistochemistry. Primary NPC and chronic nasopharyngitis (CNP) tissue samples were acquired from Nanjing First Hospital. Immunohistochemistry (IHC) slice sections were deparaffinized for 10 min, subjected to two changes of xylene, and hydrated using an ethyl alcohol gradient. For recovering antigenic sites, the sections were placed in 10mM pH6 citrate for 3 min at 116°C. Tissue staining was performed in accordance with the manufacturer's instructions using the UltraSensitive™ SP IHC Kit. Anti-TXNRD1 and anti-RASSF1A antibodies were used as the primary antibodies. DAB was used for rapid color

development. Semi-quantitative analysis of protein expression levels was conducted using Image-Pro Plus software (version 6.0; Media Cybernetics, Bethesda, MD, USA) after eliminating false-positive immunohistochemistry staining. The area and integrated optical density (IOD) values of the positive-expression sections were measured. The positive-expression sections' area and integrated optical density (IOD) values were calculated. The IOD/area value reflects the protein expression levels as well as the density of dye staining (Supplementary Figures S2, S3).

This study was reviewed and approved by Nanjing First Hospital, Nanjing Medical University, Nanjing, China (DWSY-2100345).

Kaplan-Meier plotter analysis. The TCGA database, which integrates clinical data and gene expression, and the Kaplan-Meier Plotter, were used to study the clinical relevance of TXNRD1 expression linked to SCCHN patient survival. A total of 518 patients with SCCHN were selected and divided into two groups based on low or high TR1 expression. Log-rank test p-values were estimated, with statistical significance set at $p < 0.05$.

Statistical analysis. GraphPad Prism 9 was used to analyze data, which are expressed as mean \pm SD (La Jolla, CA, USA). The one-way analysis of variance (ANOVA) and Bonferroni's multiple comparison test were used to compare multiple groups, while the Student's t-test was utilized to compare two groups. Statistics were considered significant when $p < 0.05$. (* $p < 0.05$; ** $p < 0.01$, *** $p < 0.001$, **** $p < 0.0001$).

Results

RASSF1A expression is decreased in NPC cell lines and tissues of NPC patients. WB experiments indicated that RASSF1A expression in the NPC cell lines C666-1, HONE1, and CNE1 was lower than that in the normal intestinal epithelial cell line (FHC), and that C666-1, which is a RASSF1A-deficient cell line, barely expressed RASSF1A (Figures 1A, 1B). IHC experiments showed that RASSF1A expression in tissue sections from patients with NPC was significantly lower than that in patients with CNP (Figures 1C, 1D). Moreover, the overall survival (OS) rate of a low-RASSF1A-expression patient group was lower than that of a high-RASSF1A-expression SCCHN patient group (Figure 1E). These data suggested that RASSF1A expression in NPC tissues was significantly lower than that in normal epithelial tissues and in patients with CNP. This suggested that low RASSF1A expression may predict a worse prognosis for patients with NPC.

RASSF1A overexpression sensitizes C666-1, HONE1, and CNE1 cells to radiotherapy. To demonstrate the critical effects exerted by RASSF1A on the radiation sensitivity of NPC cells, we established C666-1-RASSF1A, HONE1-RASSF1A, and CNE1-RASSF1A cells that stably overexpressed RASSF1A (Figures 2A, 2B), and subjected them to different doses of radiation (0, 2, 4, 6, and 8 Gy). At first,

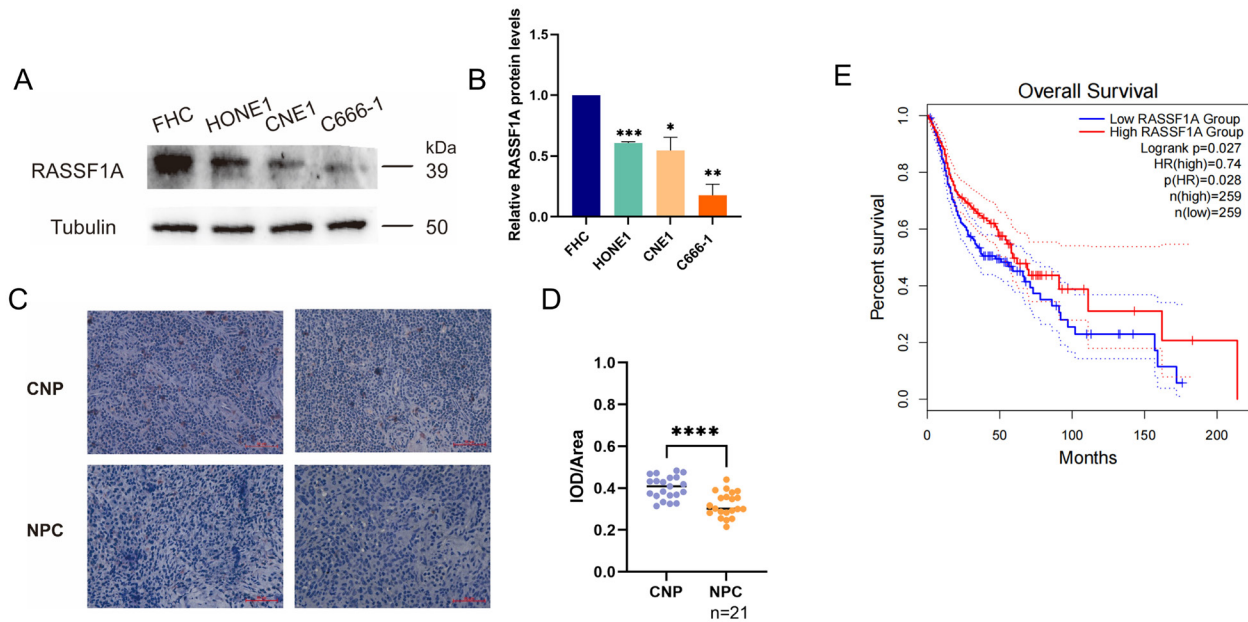


Figure 1. RASSF1A expression is decreased in NPC cell lines and NPC patients' tissue and is associated with the overall survival rate of SCCHN. A, B) Western blotting analysis of RASSF1A protein expression in normal intestinal epithelial cell line (FHC) and three NPC cell lines (CNE1, HONE1, and C666-1). Tubulin was used as an internal control. These data are representative of three independent experiments. Mean \pm SD (n=3); Student's t tests; *p<0.05; **p<0.01; ***p<0.001; ****p<0.0001. C, D) NPC and CNP paraffinized sections (400 \times) were used for IHC of the protein levels of RASSF1A. Scale bar: 50 μ m. Abbreviation: IOD-integrated optical density. E) Correlation of the expression levels of RASSF1A with the prognosis of NPC patients. Kaplan-Meier analyses for OS of SCCHN patients based on RASSF1A expression. Log-rank test was used to calculate the p-values.

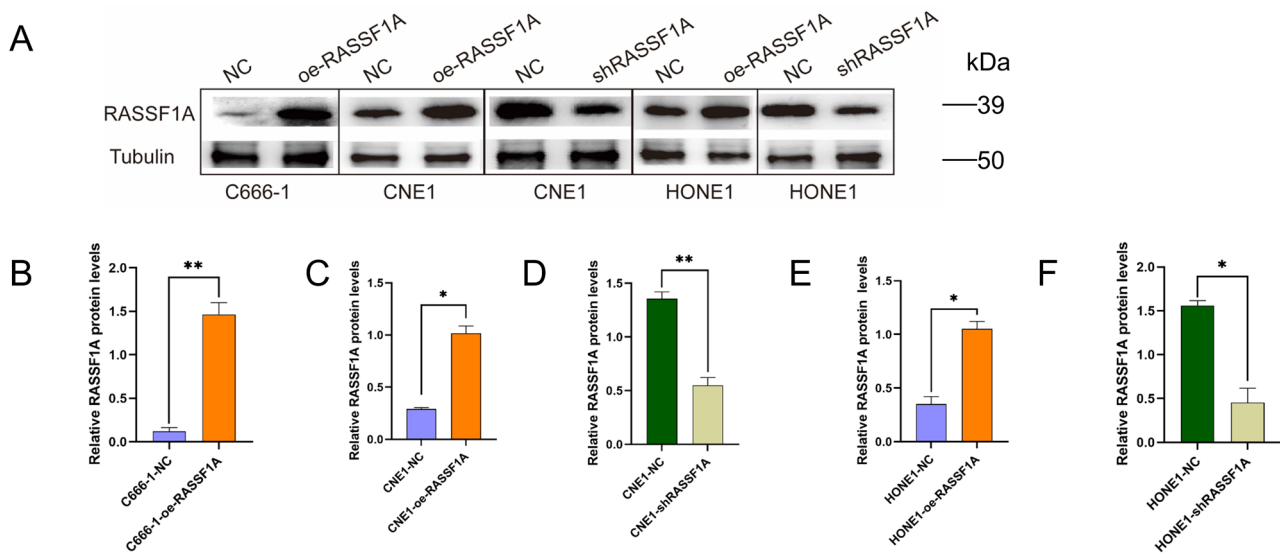


Figure 2. Effects of RASSF1A overexpression and knockdown were confirmed by western blotting. A) Effects of RASSF1A overexpression and knockdown were confirmed by western blotting. Tubulin was used as an internal control. These data are representative of three independent experiments. B–F) Evaluating the relative level of each protein expression through ImageJ software. These data are representative of three independent experiments. Mean \pm SD (n=3); Student's t-tests; *p<0.05; **p<0.01

all cells exposed to increasing doses of radiation showed a valid decrease in proliferation. The CCK-8 assay showed that the proliferation of C666-1, HONE1, and CNE1 cells overexpressing RASSF1A was significantly inhibited by different doses of radiation, compared to that of cells trans-

ected with an empty plasmid (Figures 3A, 3B, 3D, 4A, 4C, 4D). Similarly, in the clone formation assay, overexpression of RASSF1A greatly increased the sensitivity of NPC cell lines to radiotherapy and decreased their colony formation ability (Figures 3C, 3E, 4B, 4E). Meanwhile, the proliferative

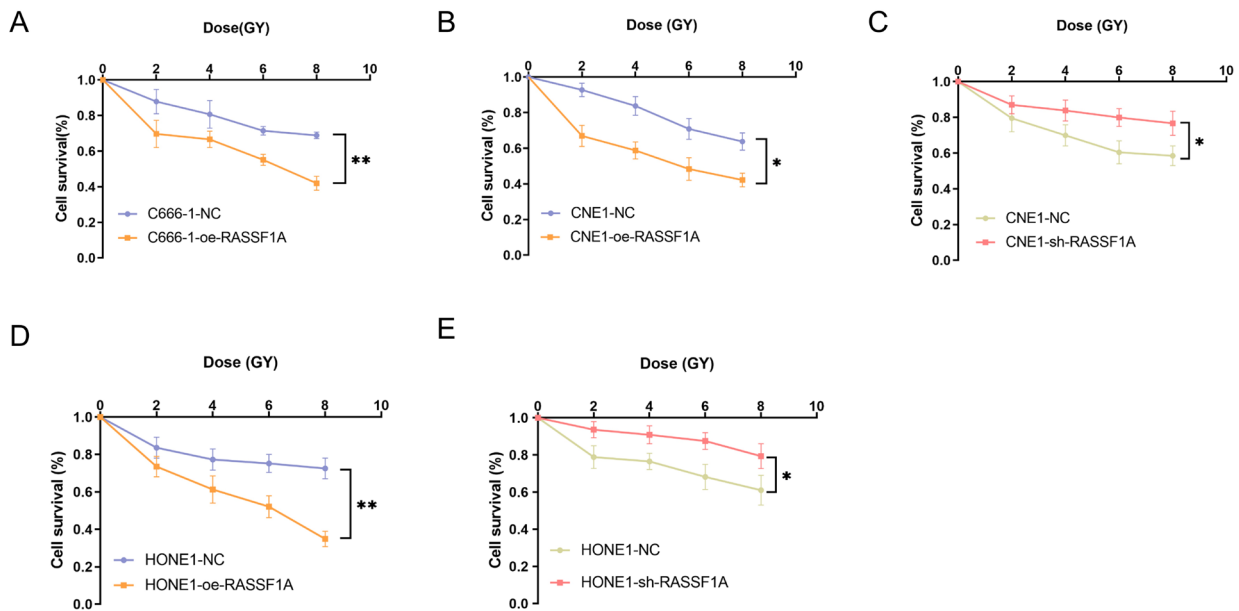
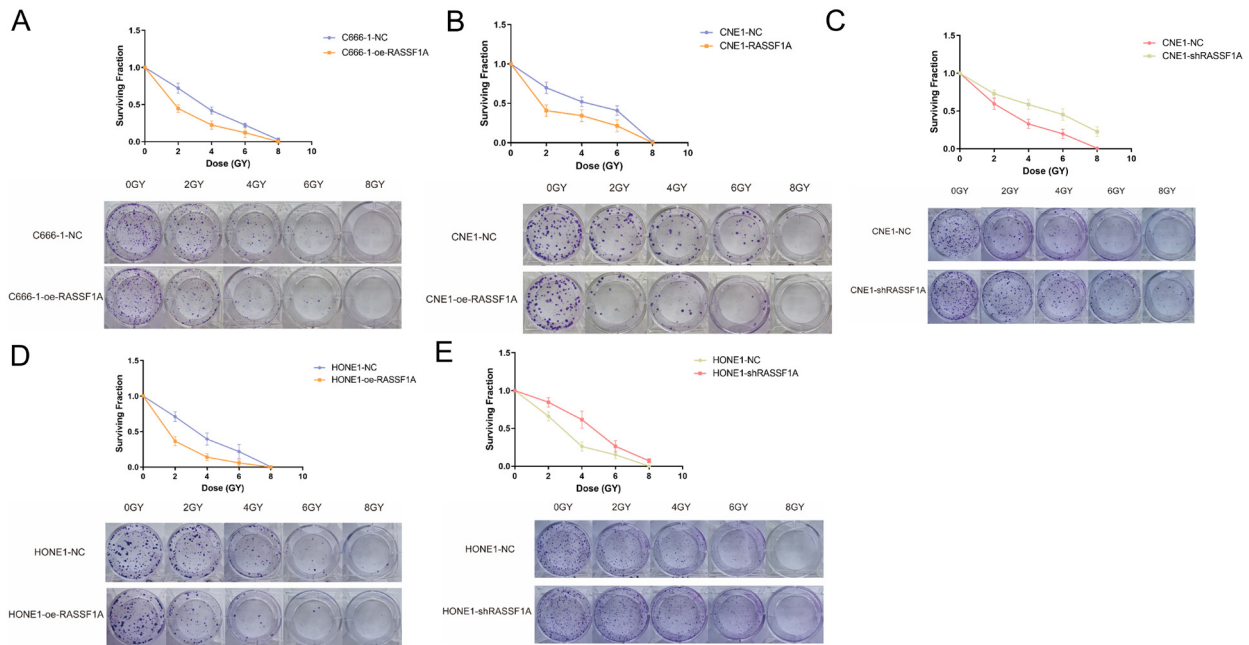


Figure 3. RASSF1A overexpression sensitizes C666-1, HONE1, and CNE1 cells to radiotherapy. A–E) CCK-8 assay was performed to evaluate cell survival in RASSF1A-knockdown and -overexpressing cells after exposure to the indicated radiation doses (0, 2, 4, 6, 8 Gy) and culture for 48 h subsequently. These data are representative of three independent experiments. Mean \pm SD (n=3); two-way ANOVA and Tukey multiple comparison tests; *p<0.05; **p<0.01



capacity of CNE1-shRASSF1A and HONE1-shRASSF1A cells was found to be increased. Considered together, our results confirmed that RASSF1A overexpression greatly increased the radiotherapy sensitivity of the NPC cell lines, C666-1, HONE1, and CNE1.

RASSF1A overexpression inhibits the expression of TXNRD1 *in vitro*. Radiotherapy may elevate ROS levels in cancer cells, leading to oxidative stress and subsequent tumor cell death. TXNRD1 reduces the occurrence of oxidative stress by inhibiting ROS. We speculated that RASSF1A may

promote sensitivity of NPC to radiotherapy by inhibiting TXNRD1 expression, and thus examined TXNRD1 expression in cells with high/low expression of RASSF1A before and after radiotherapy. TXNRD1 expression in NPC cells with high RASSF1A expression decreased. TXNRD1 expression in NPC cells with low RASSF1A expression was significantly increased (Figures 5A–5E). These results demonstrate that high expression of RASSF1A may inhibit TXNRD1 expression, thus improving the sensitivity of NPC to radiotherapy.

RASSF1A expression is correlated with that of TXNRD1 in patient tumor tissues. IHC of tissue sections from patients with NPC revealed that TXNRD1 expression was weaker in tumor tissues from patients with high RASSF1A expression, whereas TXNRD1 expression was higher in tumor tissues from patients with low RASSF1A expression. Therefore, we inferred that RASSF1A expression was correlated with that of TXNRD1 in NPC samples and that overexpression of RASSF1A may effectively suppress TXNRD1 expression (Figures 6A, 6B).

AGP enhances the sensitivity of NPC cells to radiotherapy by elevating intracellular ROS levels *in vitro*. Because RASSF1A overexpression promotes the sensitivity of NPC to radiotherapy, we investigated whether AGP, which promotes RASSF1A expression (Figure 7A), would induce a

similar effect *in vitro*. The CCK-8 assay demonstrated that the proliferation of tumor cells treated with AGP was significantly inhibited following radiotherapy (Figure 7B). Furthermore, the clone formation assay indicated that AGP combined with radiotherapy effectively inhibited tumor cell proliferation (Figure 7C). These results demonstrated that AGP combined with radiotherapy would effectively induce cancer cell death. AGP also significantly inhibited the expression of TXNRD1 (Figure 7D). Considering that activated Nrf2 signaling reportedly inhibits ROS production, we analyzed the levels of intracellular ROS in HONE1-NC, HONE1-AGP (5 μ M), HONE1-NC/4GY, and HONE1-AGP/4GY cells (Figure 7E). The induction of intracellular ROS upon AGP treatment led to marked sensitization to radiotherapy. These results indicated that AGP overexpressed RASSF1A sensitizes NPC cells to radiotherapy by elevating intracellular ROS levels.

RASSF1A overexpression sensitizes C666-1, HONE1, and CNE1 to radiotherapy by promoting FoxO3a expression and inhibiting the Nrf2/TXNRD1 signaling pathway. The expression of FoxO3a was significantly elevated in the nuclear proteins of AGP-treated HONE1 and HONE1-RASSF1A cells. Simultaneously, Nrf2 expression in the nuclei of HONE1-RASSF1A cells increased, while its expression in the cytoplasm decreased (Figures 8A–8C). Similar

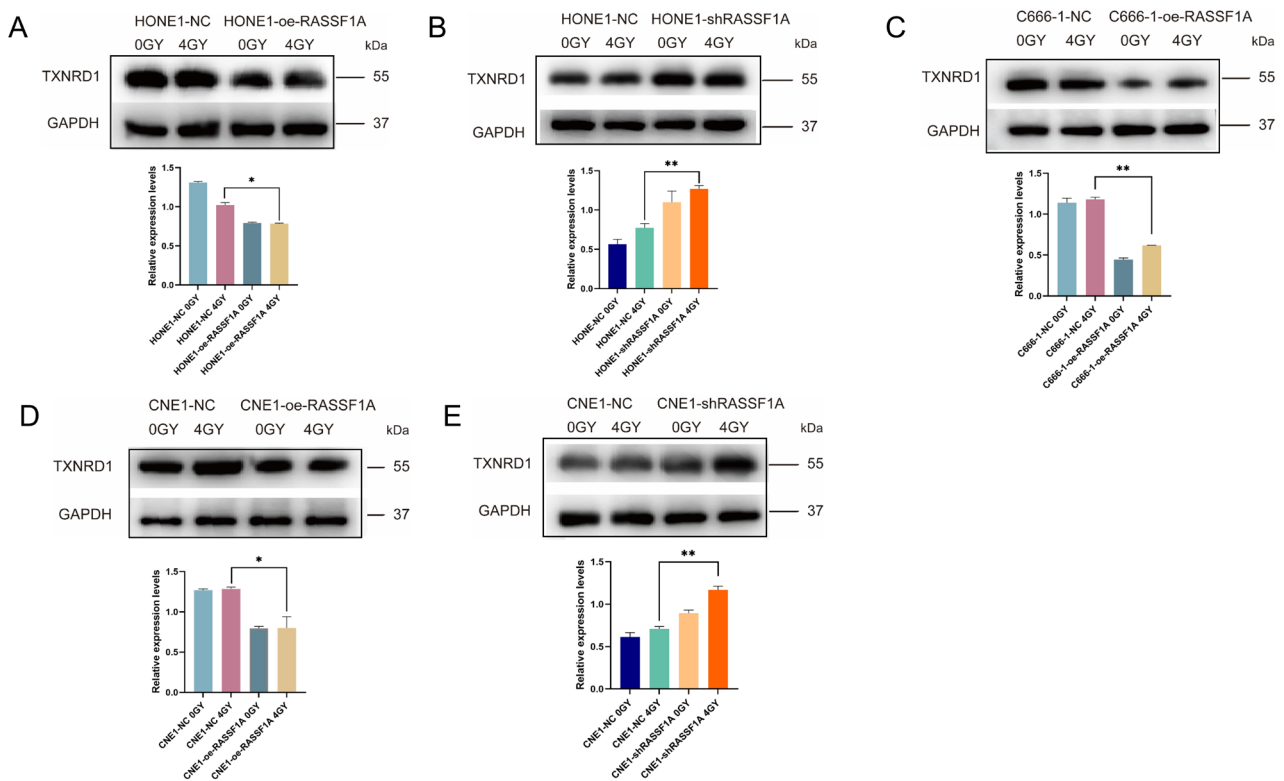


Figure 5. RASSF1A inhibits the expression of TXNRD1 in NPC cells. A–E) Expression of TXNRD1 was detected in RASSF1A-overexpressing/RASSF1A-knockdown or control cells after radiation exposure (4 Gy) and culture for 24 h subsequently. These data are representative of three independent experiments. Mean \pm SD (n=3); Student's t-tests; *p<0.05; **p<0.01

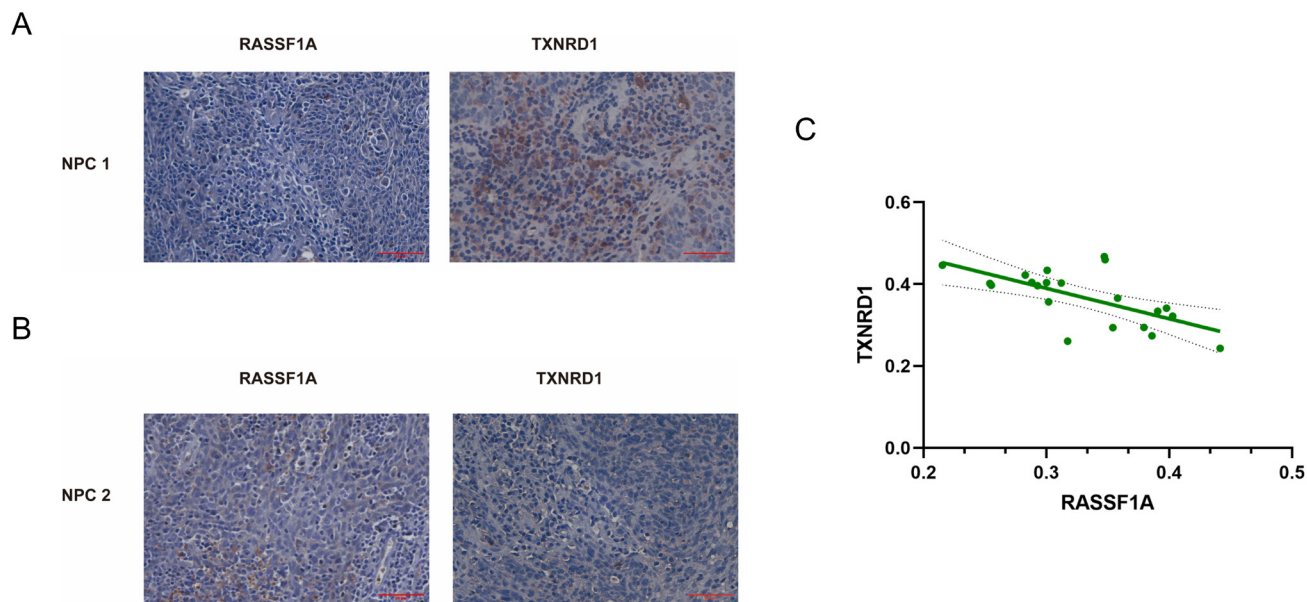


Figure 6. Expression of RASSF1A correlates with that of TXNRD1 in patient tumor tissues. A, B) NPC paraffinized sections (400×) were used for IHC of the protein levels of RASSF1A and TXNRD1. Scale bar: 50 μm. C) The expression of RASSF1A correlates with TXNRD1 in patient samples.

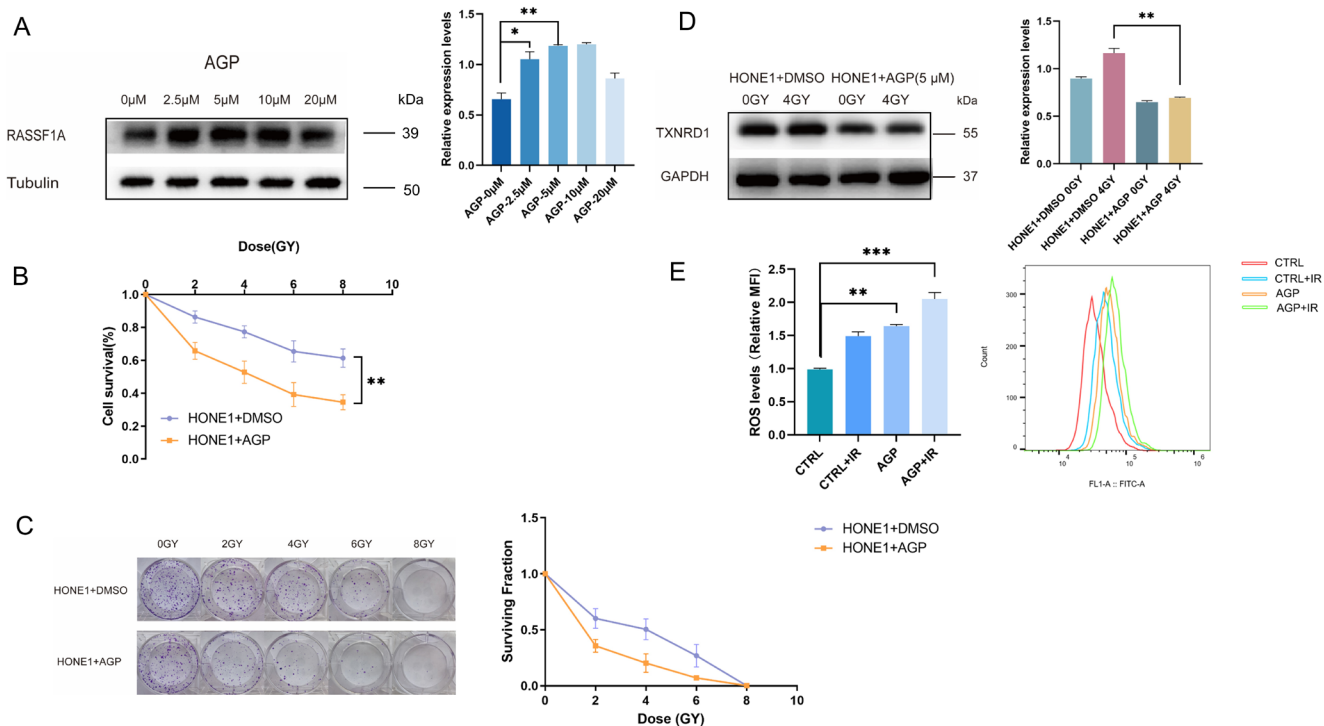


Figure 7. AGP enhances the sensitivity of NPC cells towards radiotherapy and inhibits expression levels of TXNRD1 *in vitro*. A) AGP can promote the expression of RASSF1A, with the best effect at the concentration of 5 μM. B, C) CCK-8 assay and colony formation assay were performed to evaluate cell survival in RASSF1A-AGP (5 μM) and or control cells after exposure to the indicated radiation doses (0, 2, 4, 6, 8 Gy). D) Expression of TXNRD1 was detected in RASSF1A-AGP or control cells after radiation exposure (4 Gy) and culture for 24 h subsequently. E) Flow cytometric analysis of intracellular ROS levels.

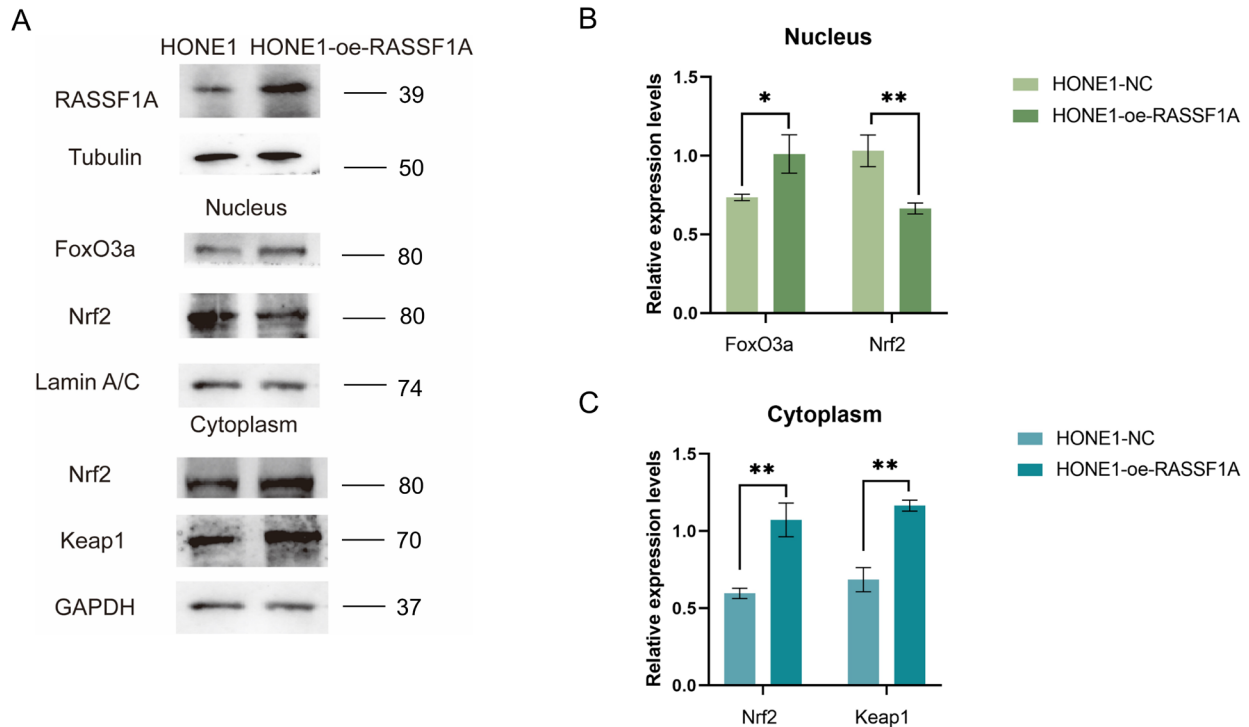


Figure 8. RASSF1A overexpression sensitizes HONE1 to radiotherapy by promoting FoxO3a and inhibiting the Nrf2/TXNRD1 signaling pathway. A) Protein levels of FoxO3a, Keap1, and Nrf2 in the nucleus and cytoplasm of HONE1-RASSF1A and HONE1-NC cells were detected by western blot. B, C) Quantitative representation of blot band intensities measured using ImageJ software. Data are expressed as the mean \pm SD, and the results represent three independent experiments.

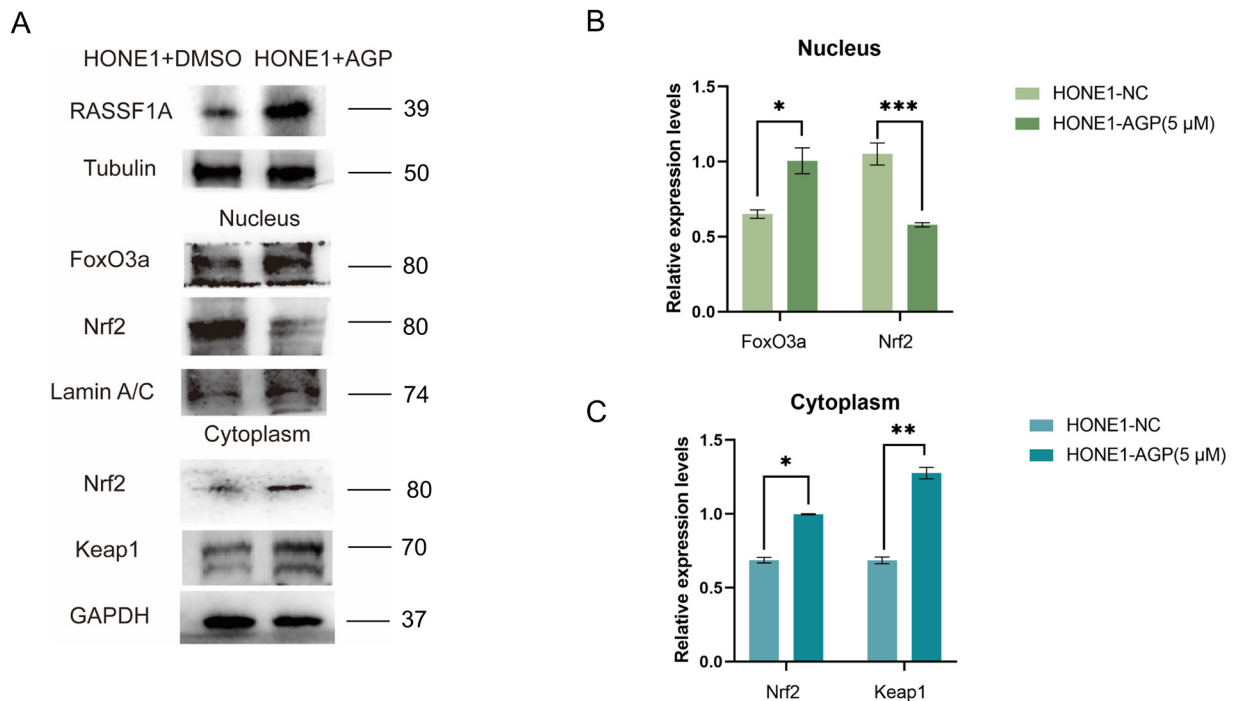


Figure 9. AGP treatment sensitizes HONE1 to radiotherapy by promoting FoxO3a and inhibiting the Nrf2/TXNRD1 signaling pathway. A) Protein levels of FoxO3a, Keap1, and Nrf2 in the nucleus and cytoplasm of HONE1-AGP and HONE1-NC cells were detected by western blot. B, C) Quantitative representation of blot band intensities measured using ImageJ software. Data are expressed as the mean \pm SD, and the results represent three independent experiments.

results were also observed in AGP-treated HONE1 cells (Figures 9A–9C). These findings indicated that AGP may increase the expression of RASSF1A, which in turn promotes FoxO3a expression in the nucleus, thereby inhibiting the Nrf2 pathway and TXNRD1 expression, which in turn enhances the sensitivity of NPC cells to radiotherapy.

AGP raises the sensitivity of HONE1 cells to radiotherapy *in vivo*. The results of our *in vitro* experiments prompted us to investigate whether a combination of AGP and radiotherapy would exert a similar effect *in vivo*. Both AGP and radiotherapy individually suppressed the size of xenograft tumors. However, xenograft tumors treated with a combination of AGP and radiotherapy were significantly smaller than those treated with either AGP or radiotherapy alone (Figures 10A–10C). To determine whether the inhibition of xenograft tumors by AGP and radiotherapy was associated with TXNRD1, we performed IHC on sections of xenograft tumors. Our results indicated that TXNRD1 expression decreased after being treated with a combination of AGP and radiotherapy (Figure 10D). Therefore, it was concluded that AGP combined with radiotherapy effectively inhibits TXNRD1 expression in tumor cells, thus improving the sensitivity of NPC cells to radiotherapy.

Discussion

Although radiotherapy is recognized as a first-line treatment for NPC, the resistance shown by some patients with NPC to radiotherapy continues to pose serious challenges to clinical treatment. Therefore, a proper understanding of sensitization to therapy targets of NPC and the mechanisms underlying such therapy sensitization is crucial for decision-making associated with clinical treatment. Common mechanisms underlying resistance to radiotherapy include increased tumor size, decreased oxygen tension, and dysregulation of key genes. Thus, the exploration of sensitization to radiotherapy targets pertaining to clinical treatment may be considered vital.

RASSF1A, an oncogene, plays a significant role in many signaling pathways. Interestingly, the current study showed that viral infection may induce the loss of *RASSF1A* expression via promoter hypermethylation. This phenomenon has been observed in hepatocellular carcinoma associated with HAV, HBV, HCV, HPV infection-dependent cervical cancer, and EBV-associated NPC [14, 22]. Exogenous *RASSF1A* expression induces growth inhibition and apoptosis in tumor cell lines [23]. However, our study differs from previous

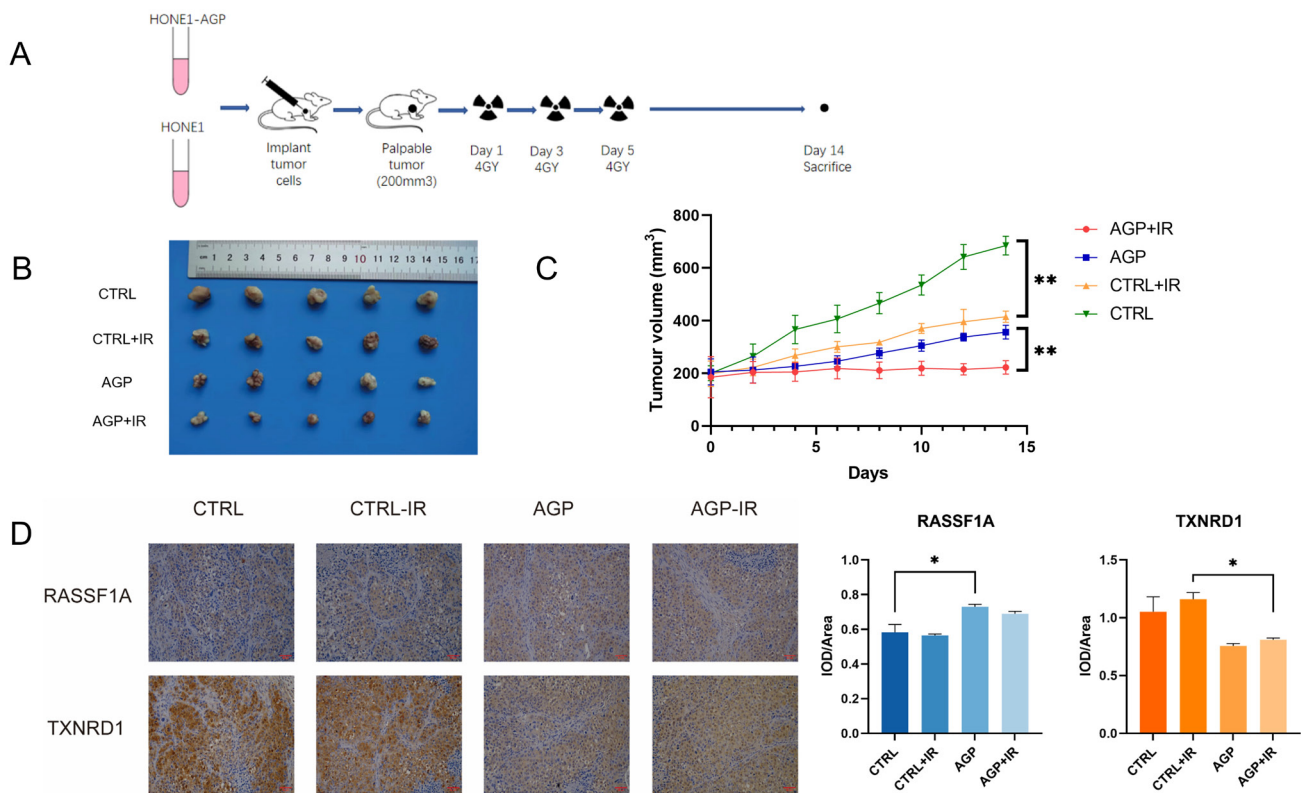


Figure 10. RASSF1A promotes radiation sensitivity in NPC cells *in vivo*. A. Schematic of the *in vivo* experiment. HONE1-NC and HONE1-AGP (μ M) were injected subcutaneously into the right flank of male nude mice. Once palpable tumors reached a volume of \sim 200 mm³, mice were subjected to radiation on days 1, 3, and 5 at a dose of 4 Gy. On day 15, the mice were euthanized, and the tumors were isolated, weighed, and compared using ANOVA. B) Representative images of xenografts from the indicated treatment groups. C) Tumor growth curves. Mean \pm SD (n=7); two-tailed t test; **p<0.01; ***p<0.001. D) Representative IHC staining images.

studies in that we focused on the effects exerted by *RASSF1A* on the sensitivity of NPC to radiotherapy leading to the finding that high *RASSF1A* expression may be considered as a sensitization target for radiotherapy, which findings also resulted in the subsequent unraveling of the mechanisms underlying this process.

Recent studies have reported that FoxO3a inactivation promotes tumorigenesis and chemoresistance in human cholangiocarcinoma via Keap1-Nrf2 signaling and that FoxO3a may reverse 5-FU resistance in colorectal cancer by inhibiting Keap1-Nrf2 [24]. These two studies link FoxO3a to the Keap1-Nrf2 pathway, providing insight into the role played by FoxO3a and the Keap1-Nrf2 pathway in cancer. However, recent studies have revealed a close relationship between Nrf2, which is a transcription factor, and cancer. The association between resistance to radiation therapy and Nrf2, in particular, is drawing attention. For example, Nrf2 plays a crucial role in the resistance shown by oral squamous cell carcinoma (OSCC) accompanied by metabolic reprogramming to radiotherapy [25]. Multiple studies have demonstrated that targeting Nrf2 is a promising strategy for enhancing radiosensitivity [26–28]. In our study, we found that *RASSF1A* may promote the sensitivity of NPC to radiotherapy by elevating the FoxO3a expression and inhibiting the Nrf2/TXNRD1 pathway. Therefore, we propose that *FOXO3a* and *Nrf2* may act as downstream genes of *RASSF1A*.

Exposure to oxidative stress causes Keap1 to undergo conformational changes which in turn induce Nrf2 dissociation. The latter protein enters the nucleus and subsequently assembles and joins muscle tenosynovial fibrosarcoma (Maf) to form a heterodimer that binds to the antioxidant response element (ARE) and triggers the transcription of several antioxidants. In response to oxidative stress, Nrf2 regulates approximately 200 cytoprotective genes, such as glutathione peroxidase (*GPX*), glutathione reductase (*GSR*), *HO-1*, superoxide dismutase (*SOD*), thioredoxin reductase (*TXNRD*), ferritin (*FTH*), *NQO1* and *TXNRD1* [29, 30]. In our study, we found that the *TXNRD1* expression in cells highly expressing *RASSF1A* was decreased significantly following radiotherapy. Moreover, Nrf2 expression among nuclear proteins was decreased. Therefore, it may be concluded that *RASSF1A* inhibits the expression of *TXNRD1* via the Nrf2/Keap1 pathway, thus promoting the production of ROS in tumor cells during radiotherapy to promote oxidative stress in cells, which kills tumor cells. Furthermore, it may be inferred that a combination of enhanced *RASSF1A* expression and radiotherapy would result in a promising strategy that may be applied at the clinical level for the purpose of improving the sensitivity of NPC to radiotherapy.

Elevated expression of *RASSF1A* may improve the sensitivity of NPC to radiotherapy. This implies that *RASSF1A* agonists may increase the therapeutic effect of radiotherapy in NPC. AGP is a traditional anti-inflammatory Chinese medicine. AGP extracted from *Andrographis paniculata* is

known to exhibit biological activities that exert anti-tumor, antibacterial, anti-inflammatory, antiviral, anti-fibrosis, immunomodulatory and hypoglycemic effects, in addition to promoting weight loss [31]. However, as an irreversible antagonist of NF- κ B [32], AGP can inhibit NF- κ B pathway. In recent studies, inhibition of NF- κ B signaling has been performed to enhance the efficacy of radiotherapy and chemotherapeutics for killing malignant cells [33]. Whether AGP promotes radiotherapy sensitization of NPC is related to the NF- κ B pathway still needs further study. In existing studies, combining classical chemotherapeutics with inhibitors of NF- κ B activation seems to result in promising synergies. Several studies have demonstrated that AGP exerts significant anti-tumor effects, such as the inhibition of proliferation and migration-related activities of various tumors. The effect of a treatment involving a combination of AGP and capecitabine on colorectal cancer was evaluated in a clinical trial. We found that the combination of AGP and radiotherapy sensitized NPC cells to radiotherapy and exerted a significant inhibitory effect *in vivo*. Thus, the combination of AGP and radiotherapy may lead to a new strategy that augments the clinical treatment of NPC.

It has been demonstrated that AGP increases nuclear Nrf2 expression and Nrf2 binding to DNA, thus promoting the antioxidant capacity of cells by increasing the levels of HO-1, glutamate cysteine ligase, and glutathione-S-transferase [34]. This prompted us to speculate that such contradictory results may be attributable to differences in the subject matter investigated by the two research studies. Our study was centered on NPC cells, in which ROS levels are higher than those of normal cells, and antioxidant defense systems are unbalanced [35]. Radiotherapy is known as a first-line treatment for NPC, while AGP is known to exert varying effects on cancer cells and normal cells by destroying cancer cells while protecting adjacent normal cells. We expect to further investigate the possibility of improving the sensitivity of NPC to radiotherapy while mitigating damage to adjacent normal cells.

In conclusion, our results indicate that *RASSF1A* may promote FoxO3a expression and inhibit Nrf2/TXNRD1 pathway-based signaling as well as TXNRD1 expression in cells, thereby enhancing the sensitivity of NPC to radiotherapy. We suggest that adjuvant-based targeting of *RASSF1A* in combination with radiotherapy may be a more effective clinical treatment strategy for NPC. AGP is a *RASSF1A* agonist that sensitizes NPC cells to radiotherapy. Thus, further clinical studies that validate AGP as an adjuvant for radiotherapy in NPC may be warranted.

Supplementary information is available in the online version of the paper.

Acknowledgments: This work was supported by the Medical Science and Technology Development Foundation of the Nanjing Department of Health [grant number YKK19079]. We are grateful to all the participants involved in this study.

References

- [1] ARSHAD S, NAVEED M, ULLIA M, JAVED K, BUTT A et al. Targeting STAT-3 signaling pathway in cancer for development of novel drugs: Advancements and challenges. *Genet Mol Biol* 2020; 43: e20180160. <https://doi.org/10.1590/1678-4685-gmb-2018-0160>
- [2] SI Y, XU J, MENG L, WU Y, QI J. Role of STAT3 in the pathogenesis of nasopharyngeal carcinoma and its significance in anticancer therapy. *Front Oncol* 2022; 12: 1021179. <https://doi.org/10.3389/fonc.2022.1021179>
- [3] CHEN YP, CHAN ATC, LE QT, BLANCHARD P, SUN Y et al. Nasopharyngeal carcinoma. *Lancet* 2019; 394: 64–80. [https://doi.org/10.1016/s0140-6736\(19\)30956-0](https://doi.org/10.1016/s0140-6736(19)30956-0)
- [4] BLANCHARD P, LEE A, MARGUET S, LECLERCQ J, NG WT et al. Chemotherapy and radiotherapy in nasopharyngeal carcinoma: an update of the MAC-NPC meta-analysis. *Lancet Oncol* 2015; 16: 645–655. [https://doi.org/10.1016/s1470-2045\(15\)70126-9](https://doi.org/10.1016/s1470-2045(15)70126-9)
- [5] SU L, SHE L, SHEN L. The Current Role of Adjuvant Chemotherapy in Locally Advanced Nasopharyngeal Carcinoma. *Front Oncol* 2020; 10: 585046. <https://doi.org/10.3389/fonc.2020.585046>
- [6] LIN Y, ZHOU X, YANG K, CHEN Y, WANG L et al. Protein tyrosine phosphatase receptor type D gene promotes radiosensitivity via STAT3 dephosphorylation in nasopharyngeal carcinoma. *Oncogene* 2021; 40: 3101–3117. <https://doi.org/10.1038/s41388-021-01768-8>
- [7] CARLOS-REYES A, MUÑOZ-LINO MA, ROMERO-GARCIA S, LÓPEZ-CAMARILLO C, HERNÁNDEZ-DE LA CRUZ ON. Biological Adaptations of Tumor Cells to Radiation Therapy. *Front Oncol* 2021; 11: 718636. <https://doi.org/10.3389/fonc.2021.718636>
- [8] CHEVALIER F. Counteracting Radio-Resistance Using the Optimization of Radiotherapy. *Int J Mol Sci* 2020; 21: 1767. <https://doi.org/10.3390/ijms21051767>
- [9] DUBOIS F, BERGOT E, ZALCMAN G, LEVALLET G. RASSF1A, puppeteer of cellular homeostasis, fights tumorigenesis, and metastasis-an updated review. *Cell Death Dis* 2019; 10: 928. <https://doi.org/10.1038/s41419-019-2169-x>
- [10] GRAWENDA A, O'NEILL E. Clinical utility of RASSF1A methylation in human malignancies. *Br J Cancer* 2015; 113: 372–381. <https://doi.org/10.1038/bjc.2015.221>
- [11] DONNINGER H, VOS M, CLARK G. The RASSF1A tumor suppressor. *J Cell Sci* 2007; 120: 3163–3172. <https://doi.org/10.1242/jcs.010389>
- [12] JIA J, WANG N, ZHENG Y, MO X, ZHANG Y et al. RAS-association domain family 1A regulates the abnormal cell proliferation in psoriasis via inhibition of Yes-associated protein. *J Cell Mol Med* 2021; 25: 5070–5081. <https://doi.org/10.1111/jcmm.16489>
- [13] ROSSWAG S, SLEEMAN J, THALER S. RASSF1A-Mediated Suppression of Estrogen Receptor Alpha (ERα)-Driven Breast Cancer Cell Growth Depends on the Hippo-Kinases LATS1 and 2. *Cells* 2021; 10. <https://doi.org/10.3390/cells10112868>
- [14] GARCIA-GUTIERREZ L, MCKENNA S, KOLCH W, MATTALLANAS D. RASSF1A Tumour Suppressor: Target the Network for Effective Cancer Therapy. *Cancers (Basel)* 2020; 12: 229. <https://doi.org/10.3390/cancers12010229>
- [15] LI J, HUANG L, HE Z, CHEN M, DING Y et al. Andrographolide Suppresses the Growth and Metastasis of Luminal-Like Breast Cancer by Inhibiting the NF-kappaB/miR-21-5p/PDCD4 Signaling Pathway. *Front Cell Dev Biol* 2021; 9: 643525. <https://doi.org/10.3389/fcell.2021.643525>
- [16] PASHA A, KUMBHAKAR DV, DONETI R, KUMAR K, DHARMAPURI G et al. Inhibition of Inducible Nitric Oxide Synthase (iNOS) by Andrographolide and In Vitro Evaluation of Its Antiproliferative and Proapoptotic Effects on Cervical Cancer. *Oxid Med Cell Longev* 2021; 2021: 6692628. <https://doi.org/10.1155/2021/6692628>
- [17] BLANCHARD TG, LAPIDUS R, BANERJEE V, BAFORD AC, CZINN SJ et al. Upregulation of RASSF1A in Colon Cancer by Suppression of Angiogenesis Signaling and Akt Activation. *Cell Physiol Biochem* 2018; 48: 1259–1273. <https://doi.org/10.1159/000492012>
- [18] MAO W, HE P, WANG W, WU X, WEI C. Andrographolide sensitizes Hep-2 human laryngeal cancer cells to carboplatin-induced apoptosis by increasing reactive oxygen species levels. *Anticancer Drugs* 2019; 30: e0774. <https://doi.org/10.1097/CAD.0000000000000774>
- [19] LIN HH, SHI MD, TSENG HC, CHEN JH. Andrographolide sensitizes the cytotoxicity of human colorectal carcinoma cells toward cisplatin via enhancing apoptosis pathways in vitro and in vivo. *Toxicol Sci* 2014; 139: 108–120. <https://doi.org/10.1093/toxsci/kfu032>
- [20] YU C, XIAO JH. The Keap1-Nrf2 System: A Mediator between Oxidative Stress and Aging. *Oxid Med Cell Longev* 2021; 2021: 6635460. <https://doi.org/10.1155/2021/6635460>
- [21] ZHOU J, DING J, MAX X, ZHANG M, HUO Z et al. The NRF2/KEAP1 Pathway Modulates Nasopharyngeal Carcinoma Cell Radiosensitivity via ROS Elimination. *Onco Targets Ther* 2020; 13: 9113–9122. <https://doi.org/10.2147/ott.S260169>
- [22] KHAN F, ALI I, AFRIDI U, ISHTIAQ M, MEHMOOD R. Epigenetic mechanisms regulating the development of hepatocellular carcinoma and their promise for therapeutics. *Hepatol Int* 2017; 11: 45–53. <https://doi.org/10.1007/s12072-016-9743-4>
- [23] WANG T, LIU H, CHEN Y, LIU W, YU J et al. Methylation associated inactivation of RASSF1A and its synergistic effect with activated K-Ras in nasopharyngeal carcinoma. *J Exp Clin Cancer Res* 2009; 28: 160. <https://doi.org/10.1186/1756-9966-28-160>
- [24] HE J, YANG Z, WU Z, WANG L, XU S et al. Expression of FOXP1 and FOXO3a in extrahepatic cholangiocarcinoma and the implications in clinicopathological significance and prognosis. *Onco Targets Ther* 2019; 12: 2955–2965. <https://doi.org/10.2147/OTT.S197001>
- [25] MATSUOKA Y, YOSHIDA R, KAWAHARA K, SAKATA J, ARITA H et al. The antioxidative stress regulator Nrf2 potentiates radioresistance of oral squamous cell carcinoma accompanied with metabolic modulation. *Lab Invest*; 202: 896–907. <https://doi.org/10.1038/s41374-022-00776-w>
- [26] WANG P, LONG F, LIN H, WANG S, WANG T. Dietary Phytochemicals Targeting Nrf2 to Enhance the Radiosensitivity of Cancer. *Oxid Med Cell Longev* 2022; 2022: 7848811. <https://doi.org/10.1155/2022/7848811>

- [27] FENG H, LIU Y, GAN Y, LI M, LIU R et al. AdipoR1 Regulates Ionizing Radiation-Induced Ferroptosis in HCC cells through Nrf2/xCT Pathway. *Oxid Med Cell Longev* 2022; 2022: 8091464. <https://doi.org/10.1155/2022/8091464>
- [28] SUN X, DONG M, GAO Y, WANG Y, DU L et al. Metformin increases the radiosensitivity of non-small cell lung cancer cells by destabilizing NRF2. *Biochem Pharmacol* 2022; 199: 114981. <https://doi.org/10.1016/j.bcp.2022.114981>
- [29] SADEGHI M, JEDDI F, SOOZANGAR N, SOMI MH, SHIRMOHAMADI M et al. Nrf2/P-glycoprotein axis is associated with clinicopathological characteristics in colorectal cancer. *Biomed Pharmacother* 2018; 104: 458–464. <https://doi.org/10.1016/j.biopha.2018.05.062>
- [30] LEE S, SELLERS B, DENICOLA G. The Regulation of NRF2 by Nutrient-Responsive Signaling and Its Role in Anabolic Cancer Metabolism. *Antioxid Redox Signal* 2018; 29: 1774–1791. <https://doi.org/10.1089/ars.2017.7356>
- [31] ZHANG H, LI S, SI Y, XU H. Andrographolide and its derivatives: Current achievements and future perspectives. *Eur J Med Chem* 2021; 224: 113710. <https://doi.org/10.1016/j.ejmech.2021.113710>
- [32] LIM JC, GOH FY, SAGINEEDU SR, YONG ACH, SIDIK SM et al. A semisynthetic diterpenoid lactone inhibits NF-kappaB signalling to ameliorate inflammation and airway hyperresponsiveness in a mouse asthma model. *Toxicol Appl Pharmacol* 2016; 302: 10–22. <https://doi.org/10.1016/j.taap.2016.04.004>
- [33] RASMI RR, SAKTHIVEL KM, GURUVAYOORAPPAN C. NF-kappaB inhibitors in treatment and prevention of lung cancer. *Biomed Pharmacother* 2020; 130: 110569. <https://doi.org/10.1016/j.biopha.2020.110569>
- [34] CHEN HW, HUANG CS, LI CC, LIN AH, HUANG YJ et al. Bioavailability of andrographolide and protection against carbon tetrachloride-induced oxidative damage in rats. *Toxicol Appl Pharmacol* 2014; 280: 1–9. <https://doi.org/10.1016/j.taap.2014.07.024>
- [35] MOLONEY JN, COTTER TG. ROS signalling in the biology of cancer. *Semin Cell Dev Biol* 2018; 80: 50–64. <https://doi.org/10.1016/j.semcdb.2017.05.023>

https://doi.org/10.4149/neo_2023_221122N1124

RASSF1A promotes radiosensitivity in nasopharyngeal carcinoma by promoting FoxO3a and inhibiting the Nrf2/TXNRD1 signaling pathway

Yishimei SI^{1,†}, Linghan MENG^{1,†}, Bingwen ZHANG^{1,†}, Yuanqing WU¹, Qianming DU², Jinjing XU^{1,*}, Jianwei QI^{1,*}

Supplementary Information

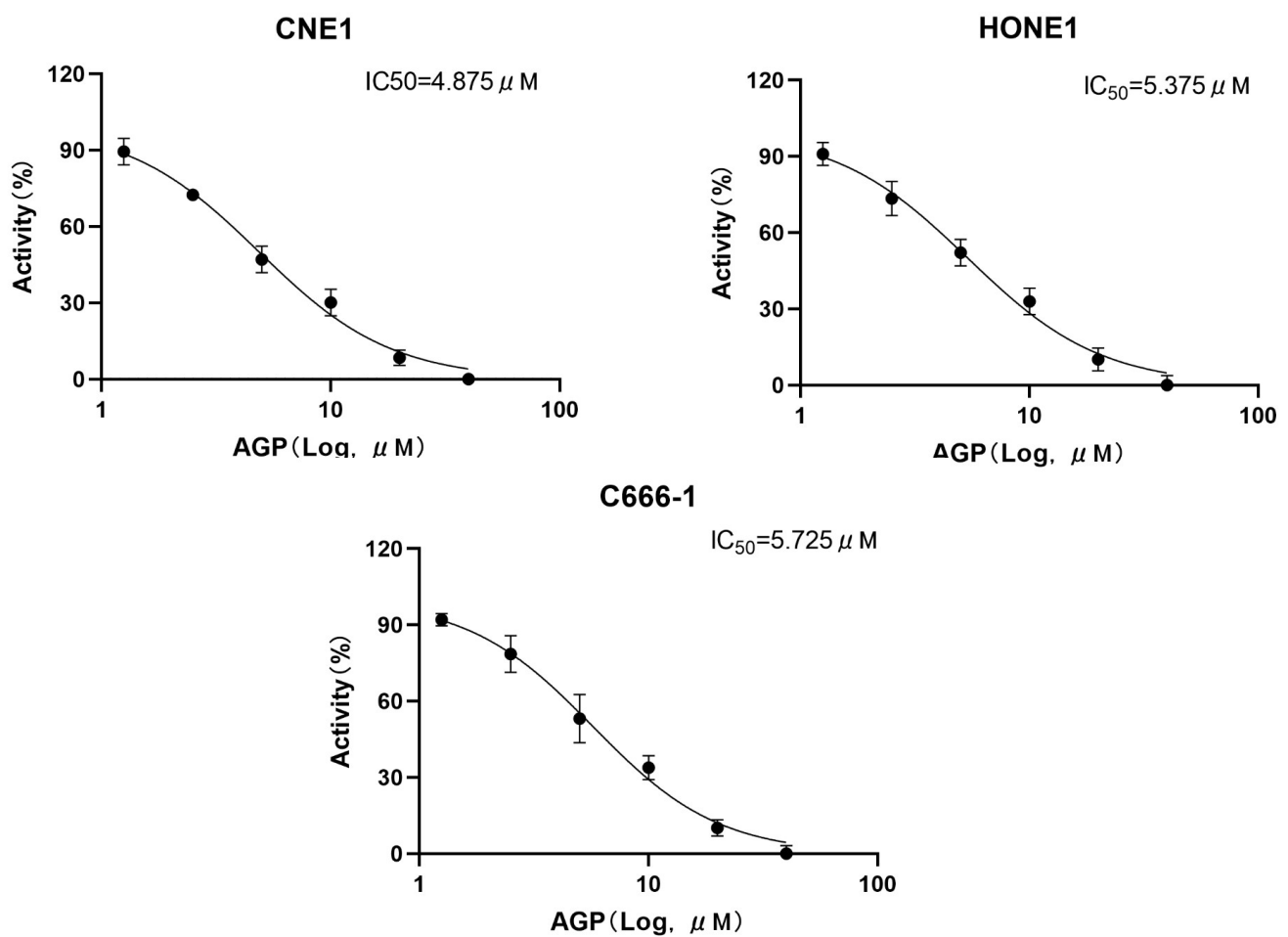


Figure S1. The analysis of IC_{50} values of 3 NPC cell lines: CNE1, HONE1, and C666-1.

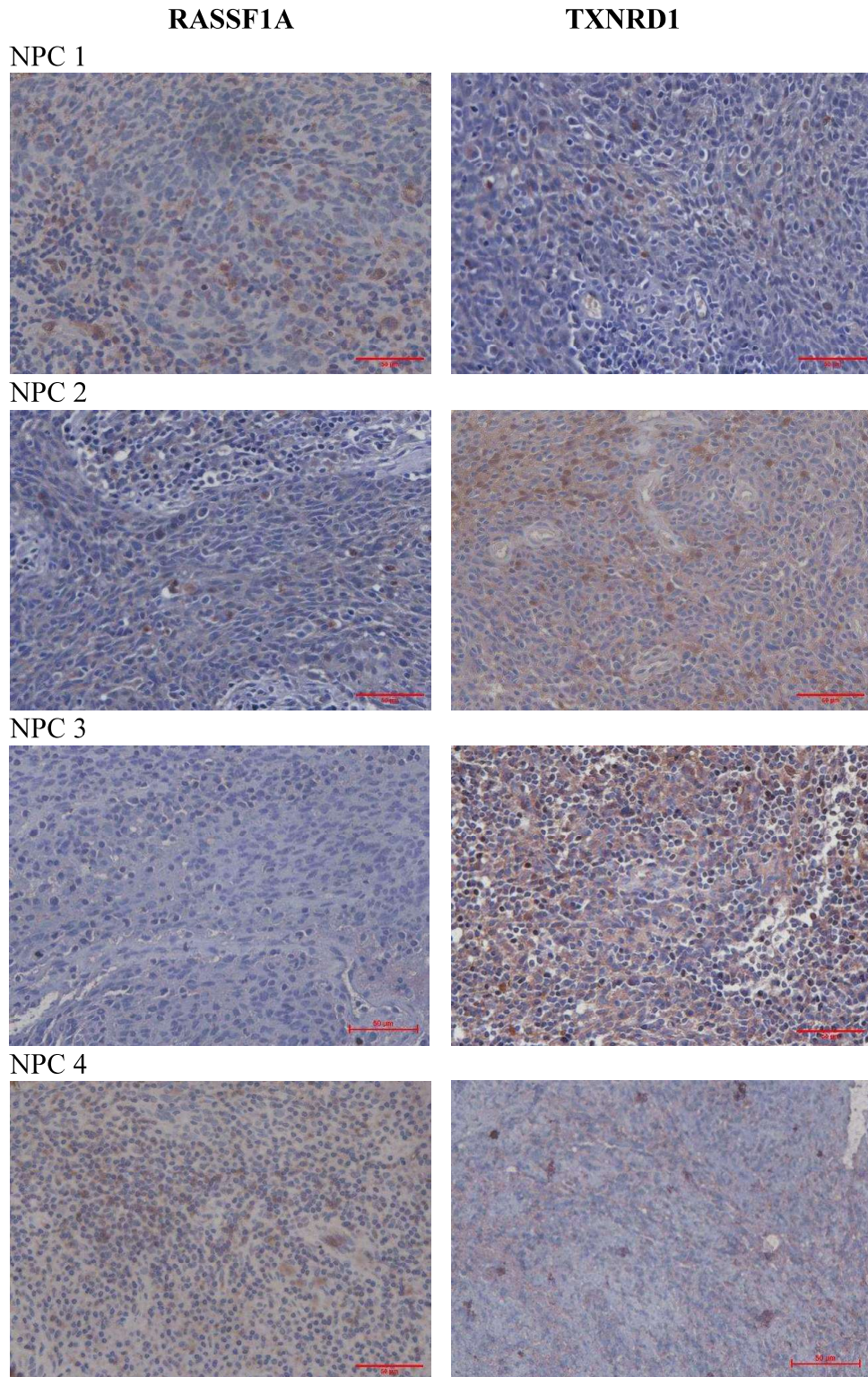


Figure S2. The expression of RASSF1A and TXNRD1 in 21 NPC patients.

Representative NPC paraffinized sections (400×) were used for IHC of the protein levels of RASSF1A and TXNRD1. Scale bar: 50 μm.

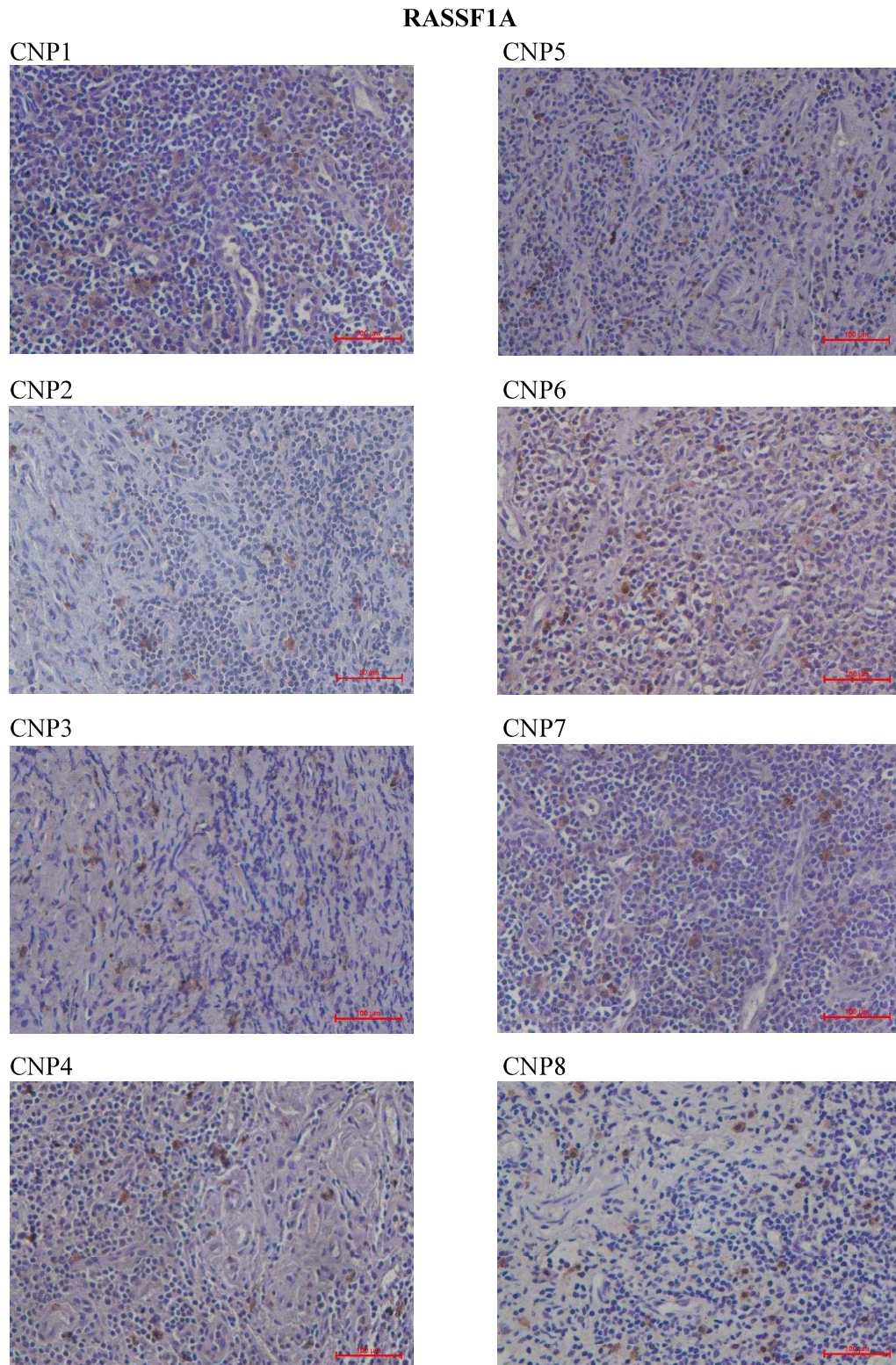


Figure S3. The expression of RASSF1A in CNP patients. Representative CNP paraffinized sections (400×) were used for IHC of the protein levels of RASSF1A. Scale bar: 50 μ m.

Supplementary Table S1. shRNA sequences of RASSF1A and the sequences of overexpression-RASSF1A.

shRASSF1A ko-1 pLKO.1 puro Sigma Aldrich TRCN0000077856		
5'-CACC	GCTTGAACAAGGACGGTTCTT	CTCGAG
CGAACTTGTTCCCTGCCAAGAA-3'		
shRASSF1A ko-2 pLKO.1 puro Sigma Aldrich TRCN0000077856		
5'-AAAC	GCTTGAACAAGGACGGTTCTT	CTCGAG
CGAACTTGTTCCCTGCCAAGAA-3'		
oeRASSF1A NM_007182.5		
5'-GAAGCTT GAATTCGCGCTAGCCATGTCGGGGGAGCC TGAG-3'		
5'-TGGGCTGGCT TACCTGCGGCCGCTTCACCCAAGGGGCA GG-3'		